J|A|C|S
ARTICLES
Published on Web 00/00/0000

Thiophene Dendron Jacketed Poly(amidoamine) Dendrimers: Nanoparticle Synthesis and Adsorption on Graphite

Suxiang Deng, Jason Locklin, Derek Patton, Akira Baba, and Rigoberto C. Advincula*

Contribution from the Department of Chemistry, University of Houston, Houston, Texas 77204-5003

Received June 29, 2004; E-mail: radvincula@uh.edu

Abstract: The peripheral functionalization of amine-terminated fourth-generation poly(amidoamine) (PAMAM) with thiophene dendrons and the preparation of dendrimer-encapsulated metal nanoparticles are described. Interesting nanoparticle stabilization and energy-transfer properties were observed with these hybrid materials. The synthesis involved imine coupling of the dendron derivatives to the peripheral amine groups of PAMAM followed by reduction. The formation of these metal−organic nanoparticle hybrid materials was monitored by UV−vis spectroscopy. The complexation of metal ions and the stabilization effect of PAMAM on metal nanoparticles were investigated by FT-IR. Energy transfer was observed between the metal surface plasmon absorption and fluorescence of the terthiophene dendrons. Noncontact magnetic-AC mode AFM imaging revealed the formation of monodispersed and very stable nanoparticles adsorbed on an HOPG flat substrate.

Introduction

As a class of macromolecules that are well defined, highly branched, and monodispersed in size, shape, and chemical composition, dendrimers have received tremendous research impetus in recent years.[1] Polyamidoamine (PAMAM) dendrimers are one of the first of a family of completely synthesized, well-characterized, and commercialized dendrimers. They are widely applied even in the biomedical field due to their excellent biocompatibility.[2] Recently, there has been a lot of interest in hybrid composites of organic and inorganic materials systems utilizing dendrimers. In particular, their role in templating nanoparticle growth has been explored. Crooks et al. have shown that PAMAM can be used as templates for preparing nearly monodispersed intradendrimer metal nanoparticles using a "ship-in-a-bottle" approach.[3] These hybrid dendrimer-encapsulated metal nanoparticles (DEMNs) are useful for applications in catalysis and electrocatalysis.[4] However, it has been difficult to immobilize and stabilize Pd DEMNs on highly ordered pyrolytic graphite (HOPG)[5] for applications such as carbon-supported electrocatalysts in the development of fuel cells.[6] This is largely due to the poor adhesion properties of the DEMNs on graphite and their strong tendency toward aggregation.

The coupling of energy and electron-transfer phenomena between inorganic nanoparticles and organic molecules is also of great interest.[7] The difference between the HOMO and LUMO levels between nanoparticles and organic dyes/conjugated polymers has resulted in both energy-transfer and quenching mechanisms. Recently, we have reported the synthesis of a new type of conjugated dendrimers based on thiophene[8] and demonstrated interesting 2-D supramolecular assembly on graphite.[9] Besides their excellent assembly properties on graphite, thiophene dendrimers also have very strong absorption in the region of 250−400 nm and are good candidates as light-harvesting antenna macromolecules.

In this paper, we report the synthesis of PAMAM dendrimers functionalized with terthiophene dendrons on their periphery (see Scheme 1) and the preparation of dendrimer-encapsulated metal nanoparticles. UV−vis spectroscopy was used to determine the number of effective binding sites for metal ions and monitor the formation of these hybrid nanoparticles. FT-IR was used to study the complexation of metal ions with functionalized PAMAM dendrimer G4(3T6C) and its effective stabilization

(1) (a) Grayson, S. M.; Fréchet, J. M. J. *Chem. Rev.* **2001**, *101*, 3819−3868. (b) Fischer, M.; Vogtle, F. *Angew. Chem., Int. Ed.* **1999**, *38*, 885−905. (c) Bosman, A. W.; Janssen, H. M.; Meijer, E. W. *Chem. Rev.* **1999**, *99*, 1665−1688. (d) Zeng, F.; Zimmerman, S. C. *Chem. Rev.* **1997**, *97*, 1681−1712. (e) *Dendrimers*; Vogtle, F., Ed.; Topics in Current Chemistry, Vol. 197; Springer: Berlin, 1998. (f) *Dendrimers II: Architecture, Nanostructure and Supramolecular Chemistry*; Vogtle, F., Ed.; Topics in Current Chemistry, Vol. 210; Springer: Berlin, 2000. (g) Emrick, T.; Fréchet, J. M. J. *Curr. Opin. Colloid Interface Sci.* **1999**, *4*, 15−23.

(2) (a) Esfand, R.; Tomalia, D. A. *Drug Discovery Today* **2001**, *6*, 427−436. (b) Zhuo, R. X.; Du, B.; Lu, Z. R. *J. Controlled Release* **1999**, *57*, 249−257.

(3) Zhao, M.; Sun, L.; Crooks, R. M. *J. Am. Chem. Soc.* **1998**, *120*, 4877−4878.

(4) (a) Zhao, M.; Crooks, R. M. *Angew. Chem., Int. Ed.* **1999**, *38*, 364−366. (b) Chechik, V.; Zhao, M.; Crooks, R. M. *J. Am. Chem. Soc.* **1999**, *121*, 4910−4911. (c) Li, Y.; El-Sayed, M. A. *J. Phys. Chem. B* **2001**, *105*, 8938−8943. (d) Stonehart, P. *Electrochemistry and Clean Energy*; The Royal Society of Chemistry: Cambridge, 1994; Vol. 146, p 17.

(5) Sun, Li.; Crooks, R. M. *Langmuir* **2002**, *18*, 8231−8236.

(6) McCreery, R. L. In *Electroanalytical Chemistry*; Bard, A. J., Ed.; Dekker: New York, 1991; Vol. 17, pp 221−374.

(7) (a) Thomas, K. G.; Kamat, P. V. *Acc. Chem. Res.* **2003**, *36*, 888−898. (b) Kamat, P. V.; Barazzouk, S.; Hotchandani, S. *Angew. Chem., Int. Ed.* **2002**, *41*, 2764−2767. (c) Pagnot, T.; Barchiesi, D.; Tribillon, G. *Appl. Phys. Lett.* **1999**, *75*, 4207−4209.

(8) Xia, C.; Fan, X.; Locklin, J.; Advincula, R. C. *Org. Lett.* **2002**, *4*, 2067−2070.

(9) Xia, C.; Fan, X.; Locklin, J.; Advincula, R. C.; Gies, A.; Nonidez, W. *J. Am. Chem. Soc.* **2004**, *126*, 8735−8743.

10.1021/ja046144l CCC: $30.25 © xxxx American Chemical Society

Scheme 1

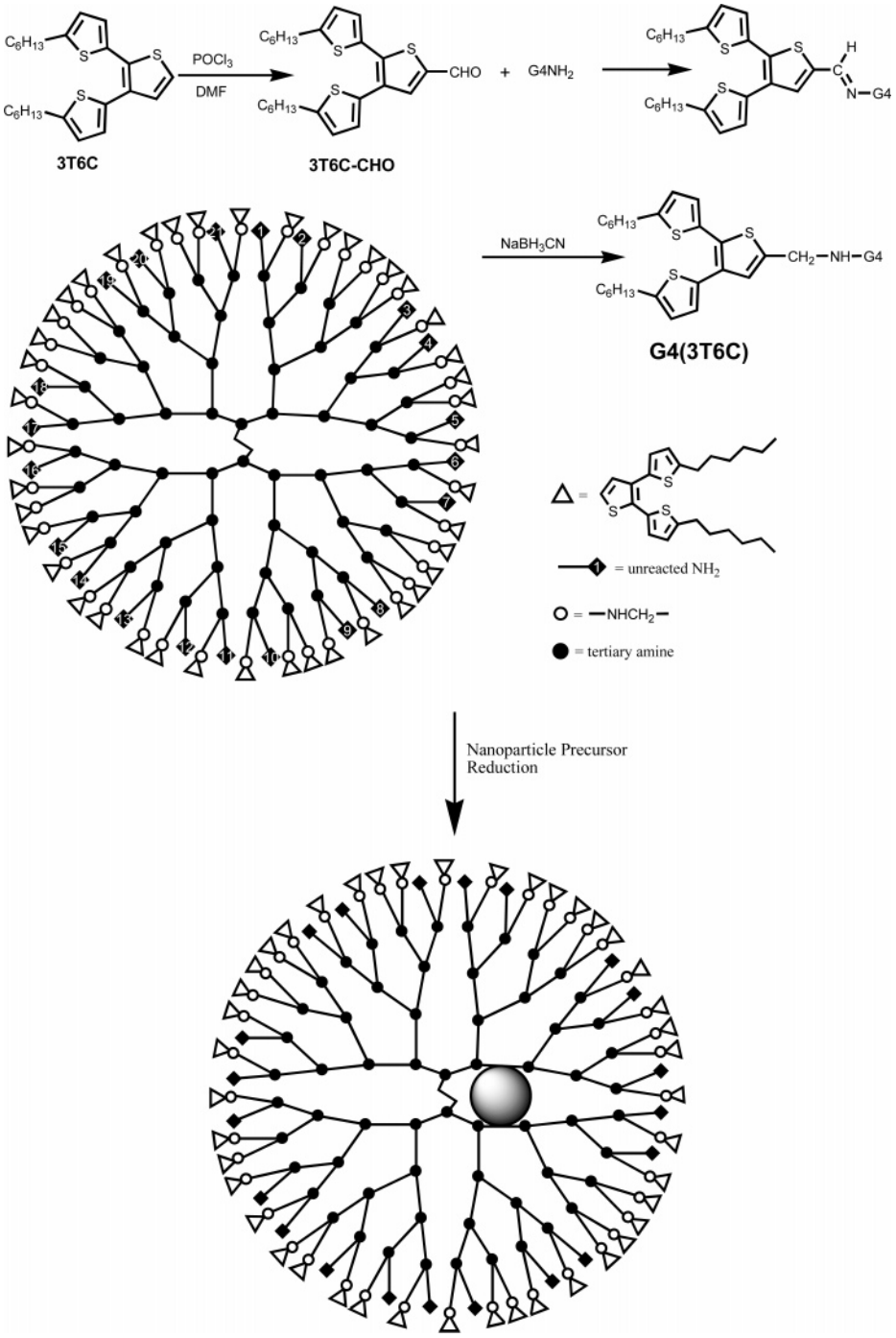

effect on the metal nanoparticles. We have investigated the energy transfer between the nanoparticles and thiophene dendron on the periphery. Finally, we studied the immobilization and stabilization of the dendrimer-encapsulated metal nanoparticles on HOPG in comparison to functionalized PAMAM dendrimer G4(3T6C).

Experimental Section

Materials. Sodium cyanoborohydride was purchased from ICN Biomedicals Inc. (Aurora, OH). Amine-terminated, fourth-generation PAMAM dendrimers ($G4NH_2$), with 64 functional amine groups in the periphery, were used as received from Aldrich. Chloroform and methanol for spectroscopic measurements were of spectrophotometric grade. All other commercially available reagents were purchased from Aldrich and used as received. Silica gel (60 Å, 32−63 μm, Standard Grade) and Alumina (Basic, Std. Activity I, 50−200 μ) were purchased from Sorbent Technologies, Inc. (Atlanta, GA). Alumina was washed with copious amounts of CH_2Cl_2 to remove any impurity and was dried before use.

Instrumentation. Nuclear magnetic resonance (NMR) spectra were recorded on a General Electric QE-300 spectrometer operating at 300 MHz for ^1H and 75 MHz for ^{13}C nuclei. UV−vis spectra were recorded on an Agilent 8453 UV−visible spectrometer, and fluorescence spectra were recorded on a Perkin Elmer LS 45 luminescence spectrometer. FT-IR spectra were obtained using a FTS 7000 spectrometer (Digilab, Randolph, MA) equipped with a liquid N_2-cooled MCT detector. KBr pellets were prepared by first mixing the sample solutions with KBr, removing solvents under vacuum, and then pressing the KBr using a

10-ton hydraulic press. Atomic force microscopy (AFM) imaging was performed in air with a PicoSPM II (PicoPlus, Molecular Imaging) in the noncontact Magnetic AC mode (MAC mode). Type II MAC-levers with a spring constant of 2.8 nN/M with about 10 nm tip radius were used for all scans. Samples were prepared by dropcasting 1.0 nM solutions in $CHCl_3/CH_3OH$ (2:1, v/v) onto a freshly cleaved HOPG substrate spinning at 1000 rpm. All solutions were passed through two 0.2 μM hydrophobic fluoropore (PTFE) filters (Millex, Millipore) as they were cast. The surface was washed with deionized water, methanol, and then dried under a stream of N_2.

Synthesis of 5,5″-Dihexyl-[2,2′;3′,2″]terthiophene-5′-carbaldehyde.[10] To ice-cooled and stirred 1.22 g (8.7 mmol) of phosphorus oxychloride was added 5 mL of DMF, and the mixture was stirred for 0.5 h. A solution of 2.08 g of 5,5″-dihexyl-[2,2′;3′,2″]terthiophene (5.0 mmol) in 5 mL of DMF was added dropwise over a period of 30 min. After the completion of the addition, the mixture was gradually warmed to room temperature and then heated at 80 °C for 3 h. The mixture was then cooled and poured onto ice−water. The pH was adjusted to 6 with 5 N sodium hydroxide solution. The reaction mixture was extracted with CH_2Cl_2 (3 × 100 mL). The combined organic phases were neutralized with saturated sodium hydrogencarbonate solution, dried with $MgSO_4$, and concentrated under vacuum. The residue was subjected to silica gel column chromatography. Elution with hexane gave 0.65 g of 5,5″-dihexyl-[2,2′;3′,2″]ter-thiophene, and then elution with hexane/acetone (6/1, v/v) afforded 1.35 g (61%) of 5,5″-dihexyl-[2,2′;3′,2″]terthiophene-5′-carbaldehyde. ^{1}H NMR ($CDCl_3$): 9.83 (s, 1H), 7.68 (s, 1H), 7.08 (d, 1H, J = 3.3 Hz), 6.90 (d, 1H, J = 3.6 Hz), 6.72 (d, 1H, J = 3.3 Hz), 6.69 (d, 1H, J = 3.6 Hz), 2.78 (m, 4H), 1.65 (m, 4H), 1.33 (m, 12H), 0.90 (m, 6H). ^{13}C NMR (300 MHz, $CDCl_3$): δ 182.3, 149.4, 147.3, 142.6, 139.7, 139.0, 132.8, 132.1, 131.4, 128.4, 127.2, 124.5, 124.2, 31.44, 31.41, 31.35, 31.25, 30.01, 29.98, 28.56, 22.42, 22.39, 13.89, 13.87.

Synthesis of Thiophene Dendron-Functionalized PAMAM Dendrimer G4(3T6C).[11] $G4NH_2$ was reacted with a 2-fold excess (128 equiv based on the 64 dendrimer terminal groups) of 5,5″-dihexyl-[2,2′;3′,2″]terthiophene-5′-carbaldehyde in dry CH_2Cl_2/CH_3OH (1:1, v/v). The reaction was allowed to proceed for 5 days at room temperature under nitrogen. A 5-fold excess of $NaBH_3CN$ (320 equiv based on the 64 dendrimer terminal groups) was added in five portions during 4 h. After addition, the reaction mixture was refluxed for 6 h and concentrated under vacuum. Workup consisted of the addition of 10% HCl to pH 5, with stirring overnight, filtration, and concentration. The residue was partitioned between saturated aqueous K_2CO_3 and CH_2Cl_2. The aqueous phase was extracted with CH_2Cl_2, and the organic phases were combined, dried with $MgSO_4$, and concentrated. The resulting residue was subjected to chromatography on alumina. Copious amounts of CH_3OH were used to wash out any impurity. The alumina was dried and extracted repeatedly with CH_2Cl_2 using a Soxhlet extractor. The extract was concentrated, and the resulting thiophene dendron-functionalized PAMAM, G4(3T6C), was obtained in 35% yield as a yellow oil and found to be soluble in $CHCl_3$ and CH_2Cl_2, but not in CH_3OH. Scheme 1 shows the structure of the starting materials and the product. From ^{1}H NMR peak integration, it is estimated that about 43 terminal NH_2 groups have been functionalized (see Figure 1). An uncertainty of about 5% in the integration could mean that the number of reacted terminal NH_2 groups is as low as 41. However, MALDI mass spectroscopy analysis failed to show the molecular ion peak at 32 650. ^{1}H NMR ($CDCl_3$): 7.0−6.7 (b, 129H, 43 × 3 inner aromatic protons from the thiophene dendron 3T6C, overlapped), 6.58 (b, 86H, 43 × 2 outermost aromatic protons from 3T6C), 3.75 (t, b, 128H, $64CH_2$ from PAMAM $G4NH_2$), 3.5−1.0 (1814H, $434CH_2$ from PAMAM $G4NH_2$, $43NHCH_2$ adjacent to 3T6C, 43 × $10CH_2$ from 3T6C), 0.85 (t, b, 258H, 43 × $2CH_3$ from 3T6C). ^{13}C NMR ($CDCl_3$): δ 172.42, 147.17, 145.66, 140.47, 135.01, 132.47, 131.40, 130.50, 128.34, 127.49, 125.86, 124.09, 123.91, 52.11, 52.04, 51.88, 50.00, 37.55, 37.11, 33.89, 31.53, 30.07, 29.68, 28.75, 22.58, 14.10. FT-IR (KBr pellet): N−H stretching 3406 cm^{-1}, CH_2 stretching 2924 and 2854 cm^{-1}, amide I 1655 cm^{-1}, amide II 1547 cm^{-1}, C−H out-of-plane vibration of thiophene ring 798 cm^{-1}.

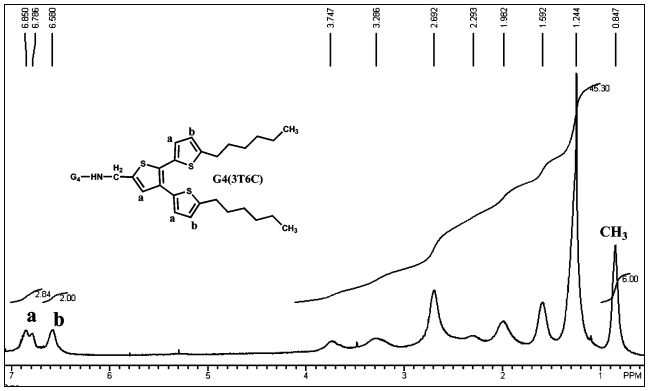

Figure 1. ^{1}H NMR of G4(3T6C). G4-NH_2 has a total of 498 CH_2, each CH_2-3T6C unit provides 11 CH_2, and only CH_3 group has a chemical shift smaller than 1.0 ppm. Therefore, by ^{1}H NMR, the number of thiophene dendron units grafted can be estimated as 996/(45.30 − 22)= 42.7 ≈ 43.

Preparation of G4(3T6C)$(Cu)_{30}$. To a reaction vial were added 1000 μL of G4(3T6C) solution (50 μM in $CHCl_3$), 333 μL of $CHCl_3$, and 667 μL of CH_3OH. With vigorous stirring, $CuCl_2$ (75 μL of 20 mM) in $CHCl_3/CH_3OH$ (2:1, v/v) was added to make a 25 μM G4(3T6C)-$(Cu^{2+})_{30}$ solution. After the mixture was stirred for 30 min, 20 equiv of $NaBH_4$ solution in $CHCl_3/CH_3OH$ (2:1, v/v, 200 mM) was added dropwise. The color of the solution changed from yellow to golden brown. The color changed slowly back to yellow in the presence of atmospheric O_2.

Preparation of G4(3T6C)$(Pd)_{24}$. To a reaction vial were added 1000 μL of G4(3T6C) solution (50 μM in $CHCl_3$), 321 μL of $CHCl_3$, and 667 μL of CH_3OH. With vigorous stirring, $Pd(OAc)_2$ (12 μL of 100 mM) in $CHCl_3$ was added to make a 25 μM G43T6C$(Pd^{2+})_{24}$ solution. After the mixture was stirred for 1 h, 20 equiv of $NaBH_4$ solution in $CHCl_3/CH_3OH$ (2:1, v/v, 200 mM) was added dropwise. The solution changed from yellow to brown after 30 min.

Preparation of G4(3T6C)$(Au)_8$. To a reaction vial were added 1000 μL of G4(3T6C) solution (50 μM in $CHCl_3$), 333 μL of $CHCl_3$, and 667 μL of CH_3OH. With vigorous stirring, $HAuCl_4 \cdot 3H_2O$ (4 μL of 100 mM) in $CHCl_3/CH_3OH$ (2:1, v/v) was added to make a 25 μM G4(3T6C)$(Au^{3+})_8$ solution. After the mixture was stirred for 1 h, 2 equiv of H_2NNH_2 solution in $CHCl_3/CH_3OH$ (2:1, v/v, 140 mM) was added dropwise. The mixture was stirred overnight. The color of the solution changed from yellow to blue.

Preparation of G4(3T6C)$(Au)_{24}$. G4(3T6C)$(Au)_{24}$ was prepared with the same procedure as that of G4(3T6C)$(Au)_8$.

Results and Discussion

Functionalization of PAMAM Dendrimer. The starting material 3T6C was synthesized as described previously.[8] We attempted to formylate 3T6C by BuLi/DMF,[12] but too many competing reactions made the purification procedure extremely difficult, resulting in a very low yield (<10%). With a Vilsmeyer formylation (see Scheme 1), a moderate yield was obtained (60%). The unreacted 3T6C can be easily recovered by elution with hexane. Moreover, except for the unreacted 3T6C, almost no byproduct was observerable by TLC using this procedure.

(10) Autorenkollektiv. *Organikum*, 19th ed.; Deutscher Verlag der Wissenschaften: Leipzig, 1993; p 343.
(11) Mickelson, J. W.; Belonga, K. L.; Jacobsen, E. J. *J. Org. Chem.* **1995**, *60*, 4177−4183.
(12) Kamerer, R. C.; Kloc, K. *J. Labelled Compd. Radiopharm.* **1987**, *24*, 1469−1477.

Scheme 2

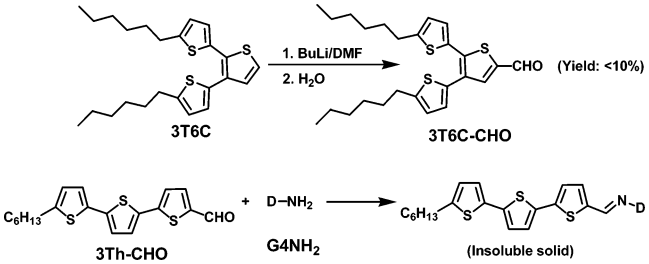

Amine-terminated, fourth-generation PAMAM dendrimers ($G4NH_2$) reacted readily with 3T6C-CHO under room temperature. Reduction of the resulting imine derivative gave a very soluble G4(3T6C). The solubility of G4(3T6C) in organic solvents, such as CH_2Cl_2 and $CHCl_3$, is very crucial for characterization, applications in nanoparticle synthesis, and thin film formation. We also functionalized $G4NH_2$ with 5″-hexyl-[2,2′;5′,2″]terthiophene-*tert*-carbaldehyde, 3Th-CHO, linear terthiophene derivative (see Scheme 2). Unfortunately, the resulting dendrimer is very insoluble in any organic solvent and thus cannot be characterized easily. As compared to 3Th-CHO, the 3T6C-CHO renders better solubility because of a less rigid nonlinear terthiophene backbone and the addition of one more hexyl chain.

The synthesis of G4(3T6C) is relatively straightforward. However, the purification was time-consuming and resulted in significant loss of product. The advantage though is that it does provide pure material. Before the addition of $NaBH_3CN$, a small amount of reaction mixture was taken out and concentrated for NMR. The imine proton resonance was observed at 8.19, and the imine carbon was observed at 172.64 ppm. After the reaction, the absence of these two peaks confirmed the complete reduction of the imine groups. The average number of thiophene dendron units grafted to PAMAM was estimated by ^{1}H NMR peak integration to be 43. An uncertainty of about 5% in the integration could mean that the number of reacted terminal NH_2 groups could be as low as 41. By contrast, there are 64 available amine groups on the periphery of PAMAM. Incomplete end-group (NH_2) functionalization was expected because of the steric hindrance. However, we anticipate that the mixed thiophene dendron/amine dendrimer periphery will provide future chemical versatility.

Dendrimer-Encapsulated Cu Nanoparticles (Cu-terthiophene PAMAM). In general, the hybrid nanoparticles can be prepared by the so-called "ship-in-a-bottle" approach.[3−5] The first step is the loading of metal ions into the interior of dendrimers. The second step is the reduction of metal ions and consequent Oswald ripening process. A solvent mixture ($CHCl_3$/CH_3OH, 2:1, v/v) was used in which the dendrimer G4(3T6C), $NaBH_4$, H_2NNH_2, and metal ions are all homogeneously soluble. This mixed solvent avoids the extra step of a heterogeneous biphasic extraction of the metal ion into the dendrimer. Each stage of preparation for the Cu hybrid nanoparticles was monitored by UV−vis spectroscopy (see Figure 2). Dendrimer G4(3T6C) does not absorb light in the range of 500−1000 nm, while Cu^{2+} alone has a broad peak centered at 920 nm corresponding to the d−d transition. In the presence of Cu^{2+}, the absorption maximum shifts to 622 nm corresponding to the d−d transition for Cu^{2+} in a tetragonally distorted octahedral or square-planar ligand field.[13,14] After reduction of Cu^{2+} with

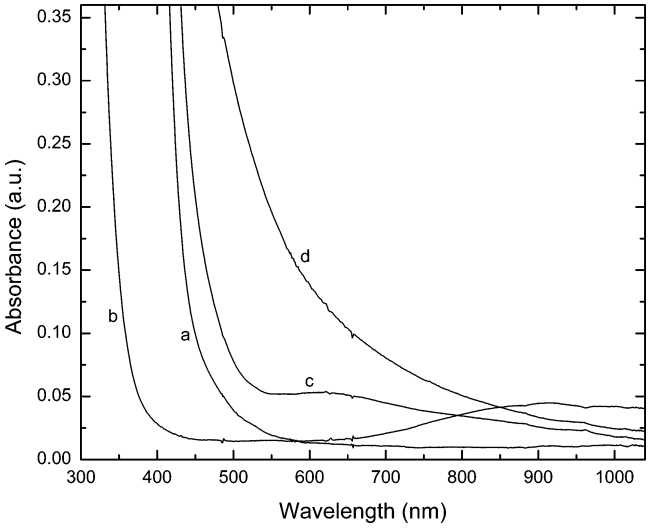

Figure 2. Absorption spectra of the dendrimers with and without Cu loading in $CHCl_3/CH_3OH$ (2:1, v/v) solutions containing: (a) 25 μM G4(3T6C); (b) 0.75 mM $CuCl_2$; (c) 25 μM G4(3T6C) and 0.75 mM $CuCl_2$; and (d) $G4(3T6C)(Cu)_{30}$.

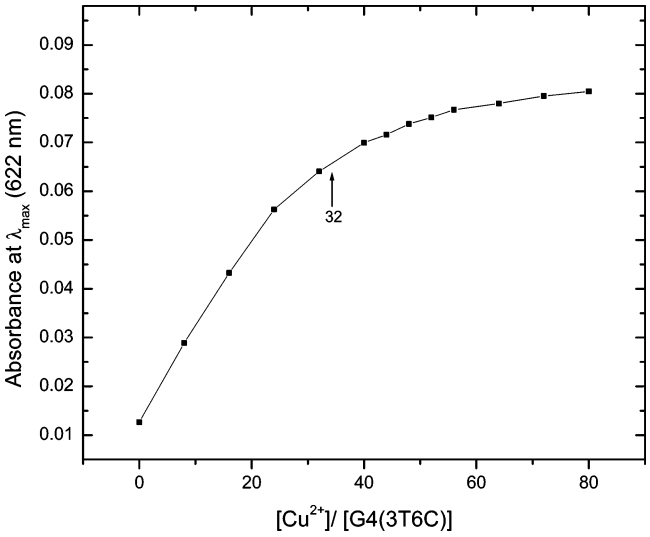

Figure 3. Spectrophotometric titration plot. The initial concentration of G4(3T6C) was 25 μM. The titration end point is estimated as the extrapolated intersection of the two linear regions of the curve before and after the equivalence point. The optical path length was 1 cm, the temperature was 20 ± 2 °C, and the solvent was $CHCl_3/CH_3OH$ (2:1, v/v).

$NaBH_4$, the d−d transition is replaced by a monotonically increasing spectrum of nearly exponential slope toward shorter wavelength[15] (see spectrum d in Figure 2), indicating the formation of Cu nanoparticles.

Determination of the Maximum Cu^{2+} Loading of G4-(3T6C). The maximum Cu^{2+} loading of G4(3T6C) was determined by titration as described in the literature.[16] Figure 3 shows the results of a titration of G4(3T6C) dendrimer with a 20 mM $CuCl_2$ solution in $CHCl_3/CH_3OH$ (2:1, v/v). As indicated by the data, G4(3T6C) adsorbs 32 Cu^{2+} ions. This number matches the number of the outermost tertiary amine. Moreover,

(13) Cotton, F. A.; Wilkinson, G. *Advance Inorganic Chemistry*, 5th ed.; Wiley & Sons: New York, 1988.
(14) Lever, A. B. P. *Inorganic Electronic Spectroscopy in Studies in Physical and Theoretical Chemistry*, 2nd ed.; Elsevier: Amsterdam, 1984.
(15) Kreibig, U.; Vollmer, M. *Optical Properties of Metal Clusters*; Springer-Verlag: Berlin, 1995.
(16) Niu, Y.; Crooks, R. M. *Chem. Mater.* **2003**, *15*, 3463−3467.

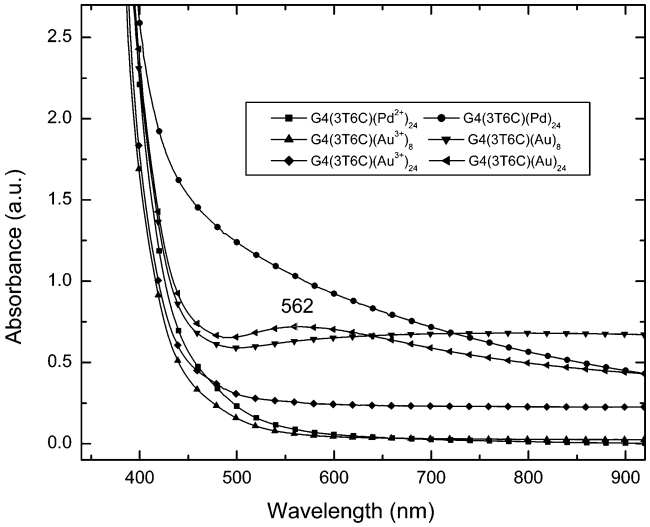

Figure 4. UV−vis absorption spectra of 25 μM dendrimer metal ion complexes and their corresponding reduced metal nanoparticles. The changes in absorption spectra of G4(3T6C)$(Pd^{2+})_{24}$ and G4(3T6C)$(Pd)_{24}$ are consistent with the formation of dendrimer-encapsulated Pd nanoparticles. The surface plasmon peak of G4(3T6C)$(Au^{3+})_8$ at about 530 nm is not observable, but is overlapped by the absorption of G4(3T6C). The surface plasmon band of the bigger Au nanoparticles G4(3T6C)$(Au^{3+})_{24}$ at 562 nm is clear.

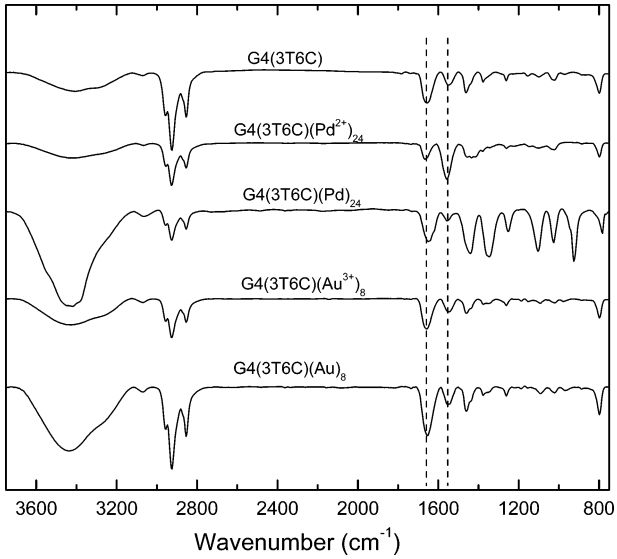

Figure 5. FT-IR spectra. Bands centered at 2924 and 2854 cm^{-1} are the CH_2 and asymmetric CH_2 stretches, and a broad band at 3400 cm^{-1} is the N−H stretch of the amino group of the dendrimers. At 799 cm^{-1} is the C−H out-of-plane vibration band of the substituted thiophene ring. The band at 1655 cm^{-1} can be assigned to amide I, while that at 1547 cm^{-1} can be assigned to amide II of the PAMAM dendrimer. Note the shift in the amide bands.

the absorption band at 622 nm is the copper d−d transition for a four-coordinated Cu(II) species with a square-planar ligand field. It seems likely that each Cu^{2+} is coordinated to two tertiary amine groups and two Cl ions. Therefore, the loading of Cu^{2+} is probably driven by interaction of Cu^{2+} with tertiary amine, not by the differential solubility of Cu^{2+} in the dendrimer interior versus the solvent.[16]

Dendrimer-Encapsulated Pd and Au (Pd and Au-terthiophene PAMAM). Pd and Au hybrid nanoparticles were also synthesized using the same approach as that for Cu. The change in absorption spectra of the dendrimers G4(3T6C)-$(Pd^{2+})_{24}$ and G4(3T6C)$(Pd)_{24}$ are consistent with the formation of dendrimer-encapsulated Pd nanoparticles. The surface plasmon peak of G4(3T6C)$(Au^{3+})_8$ at about 530 nm is not observable because of the overlap with the absorption of G4-(3T6C). Therefore, to prove the existence of Au nanoparticles inside the dendrimer, we decided to synthesize larger Au nanoparticles G4(3T6C)$(Au^{3+})_{24}$, where the surface plasmon peak at 562 nm was easily observed (see Figure 4). The resulting Pd hybrid nanoparticles are very stable. Even after several months, no agglomeration was observed and the solution spectra remained the same. However, the Au hybrid nanoparticles are not as stable as Pd. A black precipitate was formed after several weeks. This difference is discussed in the sections below.

FT-IR Spectroscopy. Each stage of preparation of the hybrid nanoparticles was also monitored by FT-IR spectra (see Figure 5). Bands centered at 2924 and 2854 cm^{-1}, and a broad band at 3400 cm^{-1}, can be assigned to the symmetric CH_2 and asymmetric CH_2 stretches,[17] and the stretching mode of the amino group of the dendrimers.[18] The C−H out-of-plane

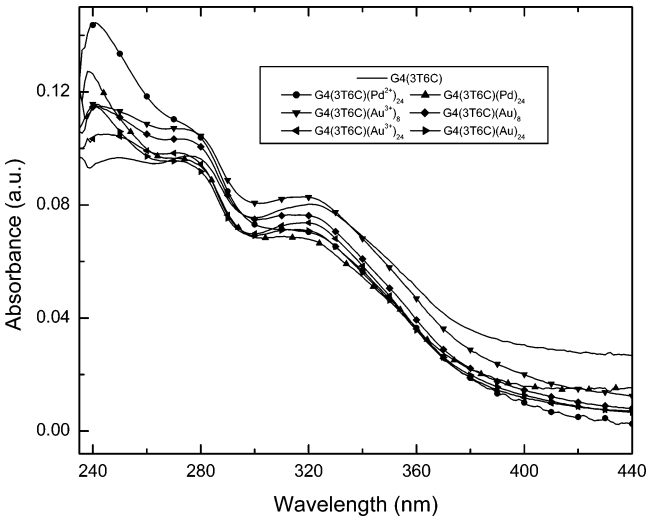

Figure 6. UV−vis absorption spectra. All the spectra are normalized to 0.1μM concentration. Dendrimer G4(3T6C) showed three characteristic absorption bands of 3T6C at about 245, 270 and 315 nm.

vibration of the substituted thiophene ring is assigned to 799 cm^{-1}.[19] Bands at approximately 1655 cm^{-1} can be assigned to amide I, and bands at 1547 cm^{-1} can be assigned to amide II of the PAMAM dendrimer.[20] Very interestingly, the loading of metal ions and presence of nanoparticles also change the amide I and II bands (see Table 1). In general, both the loading of metal ions and the presence of nanoparticles shift the amide bands to a larger wavenumber. The amide I band is more sensitive than that of amide II, and metal ions have a stronger effect than their corresponding nanoparticles. Thus, the shift of amide bands is an indication of complexation. A stronger complexation results in a larger shift. Therefore, the metal ions will complex with PAMAM more strongly than their corre-

(17) (a) Laibinis, P. E.; Bain, C. D.; Nuzzo, R. G.; Whitesides, G. M. *J. Phys. Chem.* **1995**, *99*, 7663−7676. (b) Harder, P.; Grunze, M.; Dahint, R.; Whitesides, G. M.; Laibinis, P. E. *J. Phys. Chem. B* **1998**, *102*, 426−436. (c) Porter, M. D.; Bright, T. B.; Allara, D. L.; Chidsey, C. E. D. *J. Am. Chem. Soc*. **1987**, *109*, 3559−3568.

(18) (a) Kudelski, A.; Hill, W. *Langmuir* **1999**, *15*, 3162−3168. (b) Garcia, M. E.; Baker, L. A.; Crooks, R. M. *Anal. Chem.* **1999**, *71*, 256−258.

(19) Hotta, S.; Rughooputh, S. D. D. V.; Heeger, A. J.; Wudl, F. *Macromolecules* **1987**, *20*, 212−215.

(20) Zeng, F.; Zimmerman, S. C. *Chem. Rev.* **1997**, *97*, 1681−1712.

Table 1. FT-IR Spectra Data

	amide I (cm^{-1})	shift of amide I (cm^{-1})	amide II (cm^{-1})	shift of amide II (cm^{-1})
G4(3T6C)	1655		1547	
G4(3T6C)$(Pd^{2+})_{24}$	1667	+12	1559	+12
G4(3T6C)$(Pd)_{24}$	1651	−4	1555	+8
G4(3T6C)$(Au^{3+})_8$	1659	+4	1547	0
G4(3T6C)$(Au)_8$	1655	0	1547	0
G4(3T6C)$(Au^{3+})_{24}$	1663	+8	1547	0
G4(3T6C)$(Au)_{24}$	1655	0	1547	0

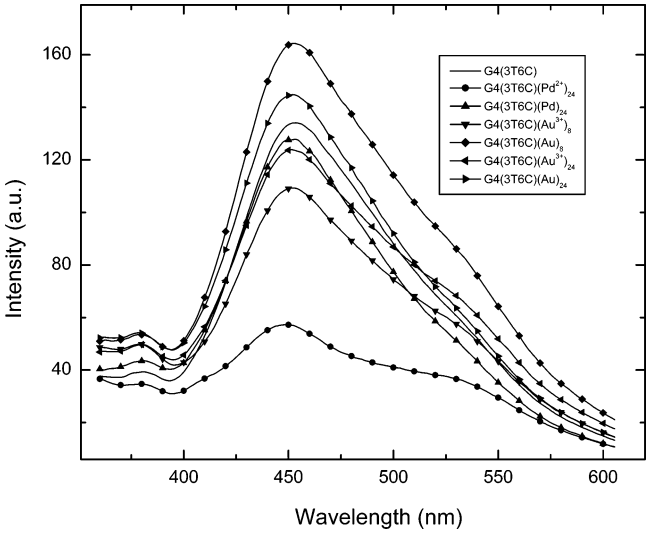

Figure 7. Steady-state fluorescence spectra. All of the spectra are normalized to a constant absorbance at the excitation wavelength 320 nm.

sponding nanoparticles. This is expected because of the electrostatic charge present on the metal ions. As indicated by the significant shift of amide bands (see Table 1), it is very clear that amide groups are involved in the complexation and stabilization of both Pd^{2+} and Pd nanoparticles, although it is not fully understood at present why the amide I of G4(3T6C)-$(Pd)_{24}$ shifts to a shorter wavenumber. However, the loading of Au^{3+} does not change the amide II band, which is a combination of C−N stretching and N−H bending. This indicates that Au^{3+} does not or very weakly binds to the NH of the amide group as compared to Pd^{2+}. Also, Au^{3+} does not shift the amide I as much as does Pd^{2+}. Therefore, amide groups do not contribute significantly to the complexation of Au^{3+} with PAMAM, partially explaining the weak complexation between Au^{3+} and PAMAM.[21] Upon the formation of Au nanoparticles, both amide I and II bands are at the exact wavenumber as for G4(3T6C). If there were weak interactions between Au^{3+} with amide groups, Au nanoparticles do not interact with it at all. This can partially explain why the Au hybrid nanoparticles are not as stable as Pd nanoparticles.

Steady-State Absorption and Fluorescence Spectroscopy. Dendrimer G4(3T6C) showed three characteristic absorption bands of 3T6C at about 245, 270, and 315 nm (see Figure 6).[9] The loading of metal ions shifts the absorption maxima to shorter wavelengths and increases the intensity of absorption at 245 nm, making the absorption peak at 270 nm not very resolvable. Upon formation of metal clusters, the absorption maxima are further blue shifted (see Table 2). This hypsochromic effect is the result of increased rigidity of the dendrimer caused by metal ions and nanoparticles. As compared to Au^{3+} and Au clusters, Pd^{2+} and Pd clusters have a stronger binding effect. This is consistent with the results from FT-IR spectra that Pd^{2+} binds more strongly to PAMAM and therefore the Pd hybrid nanoparticles are more stable. The hypsochromic effect is not obvious for fluorescence (see Table 2). Interestingly, the fluorescence of G4(3T6C) is enhanced by gold nanoparticles due to a surface

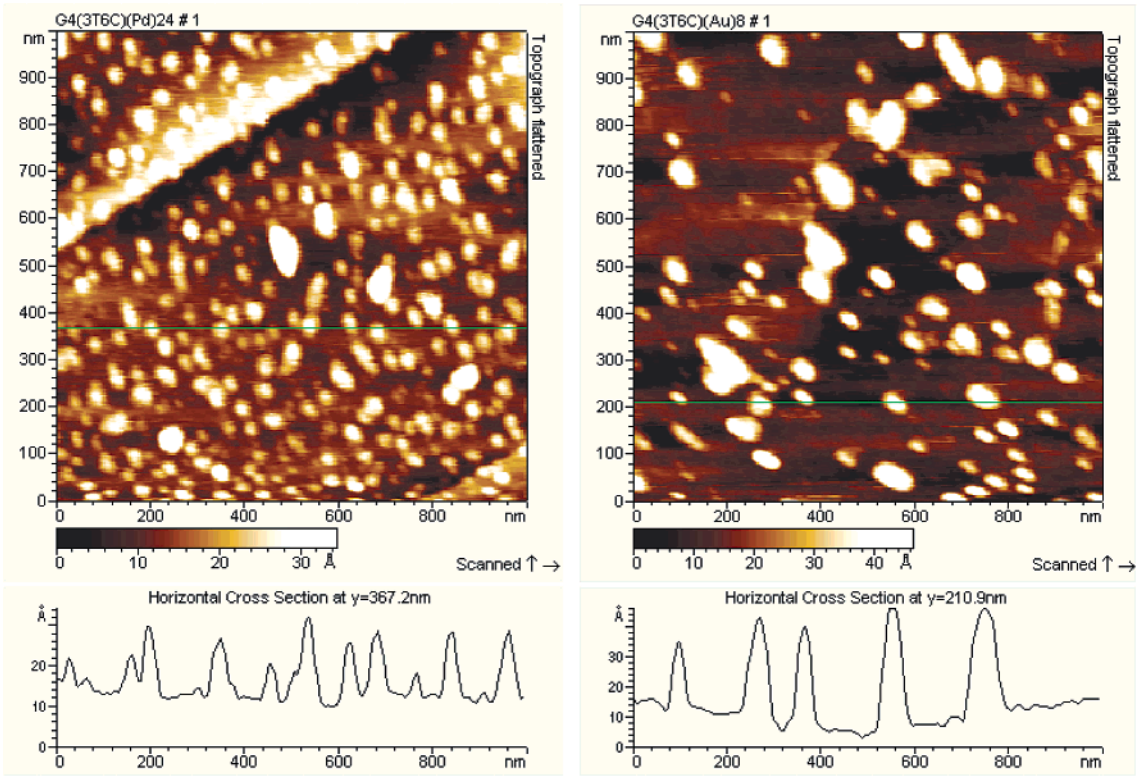

Figure 8. AFM images (1 × 1 μM) of G4(3T6C)$(Pd)_{24}$ (left) and G4(3T6C)$(Au)_8$ (right) on freshly cleaved HOPG.

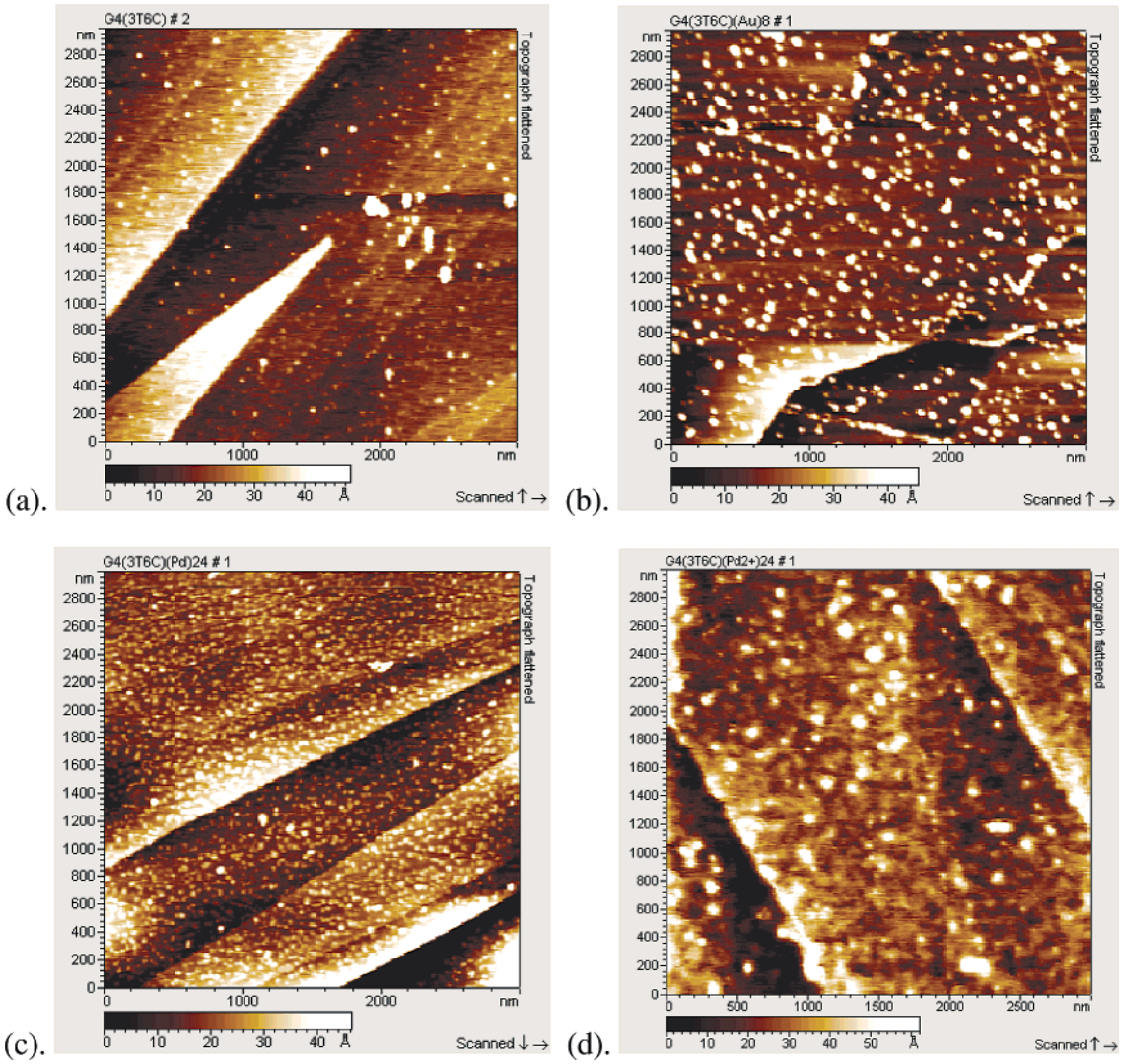

Figure 9. AFM images (3 × 3 μM) of (a) G4(3T6C), (b) G4(3T6C)$(Au)_8$, (c) G4(3T6C)$(Pd)_{24}$, and (d) G4(3T6C)$(Pd^{2+})_{24}$ on freshly cleaved HOPG.

Table 2. Extinction Coefficients, and Absorption and Fluorescence Maxima

	λ_{max}^{abs} (nm) (log ϵ)	λ_{max}^{fl} (nm)
G4(3T6C)	249 (5.99), 275 (5.99), 320 (5.90)	453.5
G4(3T6C)$(Pd^{2+})_{24}$	241 (6.16)	448.5
G4(3T6C)$(Pd)_{24}$	238 (6.10), 273 (5.98), 311 (5.84)	453
G4(3T6C)$(Au^{3+})_8$	242 (6.06), 269 (6.03), 318 (5.92)	452
G4(3T6C)$(Au)_8$	241 (6.06), 273 (6.01), 313 (5.88)	452
G4(3T6C)$(Au^{3+})_{24}$	244 (6.02), 272 (5.99), 318 (5.87)	451.5
G4(3T6C)$(Au)_{24}$	240 (6.06), 271 (5.98), 313 (5.85)	452

enhancement effect (see Figure 7).[22] The mechanism for this enhancement involves the interaction of the emission dipole moment of the gold surface plasmon resonance with the emission dipole moment of the dendrimer G4(3T6C). The surface plasmon band of G4(3T6C)$(Au)_8$ (at about 530 nm) has a better overlap with the emission of G4(3T6C) than does that of G4(3T6C)$(Au)_{24}$ (at 562 nm) (Figures 6 and 7). Therefore, the fact that G4(3T6C)$(Au)_8$ enhances the fluorescence of G4(3T6C) more than does G4(3T6C)$(Au)_{24}$ provides direct evidence for this mechanism. Surface-enhanced fluorescence is rarely observed directly in a nanoparticle and organic fluorophore system. More investigations are needed to further clarify this mechanism and compare the exact HOMO−LUMO level match.

Atomic Force Microscopy. Unlike $G4NH_2$, which can spread easily on a mica surface to form films,[23] G4(3T6C) tends to form very large aggregates. This is due to the increased hydrophobicity caused by thiophene dendrons on the periphery. However, HOPG surfaces turned out to be a very good substrate for G4(3T6C). In the AFM images of Figure 8, one can see many separate and randomly deposited globular particles on the HOPG surface. In each image, the particles appeared to be substantially uniform in size. There are a few large irregular clusters, perhaps caused by dendrimer aggregation. According to the structure of dendrimer G4(3T6C), it has approximately the same size of $G6NH_2$ (diameter ∼6.7 nm).[24] However, a strong dendrimer−graphite interaction causes a spherically symmetric dendrimer to adopt an oblate shape on the surface.[23] This is due to the strong $\pi-\pi$ stacking and interaction of the terthiophene moieties with graphite. We have recently observed

(21) Zhao, M.; Crooks, R. M. *Chem. Mater.* **1999**, *11*, 3379−3385.
(22) (a) Moskovits, M. *Rev. Mod. Phys.* **1985**, *57*, 783−826. (b) Varnavsli, O.; Ispasoiu, R. G.; Balogh, L.; Tomalia, D.; Goodson, T. *J. Chem. Phys.* **2001**, *114*, 1962−1965.
(23) Tsukruk, V. V.; Rinderspacher, F.; Bliznyuk, V. N. *Langmuir* **1997**, *13*, 2171−2176.
(24) Li, J.; Piehler, L. T.; Qin, D.; Baker, J. R., Jr.; Tomalia, D. A. *Langmuir* **2000**, *16*, 5613−5616.

this strong stabilization and order with thiophene dendrimers on HOPG as a function of dendrimer generation and alkyl chain length.[9] G4(3T6C)$(Pd)_{24}$ has an average height of 1.5 nm and full width at baseline of 50 nm. Dendrimers with metal clusters inside tend to form more uniform aggregates (see Figure 9a and b). The presence of hydrophilic metal ions may decrease the interaction between the dendrimer and hydrophobic graphite, resulting in more irregular aggregates for dendrimer loaded with metal ions (see Figure 9c and d). It should be pointed out that G4(3T6C) provides essentially a monodispersed size and strong adhesion of Pd hybrid nanoparticles to HOPG. It is very important in terms of electrocatalyst applications in fuel cells. Thus, the use of a terthiophene dendron jacketed PAMAM as a host carrier for the Pd nanoparticles is an important development for improved adsorption and stability of these catalysts on graphite electrodes. The catalytic activity of these immobilized Pd hybrid nanoparticles is currently under investigation.

Conclusions

Amine-terminated fourth-generation PAMAM dendrimers functionalized with thiophene dendrons are synthesized, and their application in the preparation of dendrimer-encapsulated nanoparticles has been demonstrated. FT-IR and UV−vis spectroscopies show evidence that Pd hybrid nanoparticles are more stable than Au nanoparticles. Fluorescence spectra indicate that thiophene dendrons interact with the encapsulated nanoparticles and their emission can even be enhanced by Au nanoparticles through energy transfer. AFM images reveal that the functionalized PAMAM dendrimer is an efficient host for immobilizing and stabilizing hybrid nanoparticles on HOPG. These Pd hybrid nanoparticles have potential application as carbon-supported electrocatalysts in fuel cells. Adsorption on nanotubes (MWNT and SWNT) is also under investigation.

Acknowledgment. We gratefully acknowledge support from various funding agencies that made this work possible: NSF-DMR-99-082010, Robert A. Welch Foundation (E-1551), NSF-CTS (0330127), NSF-DMR Instrument Grant, and NSF-CHE-0304807. Also, technical support from Digilab and Molecular Imaging is greatly acknowledged.

JA046144L